Published in final edited form as:
Neuron. 2010 September 23; 67(6): 1034–1047. doi:10.1016/j.neuron.2010.08.041.

Electrical coupling between olfactory glomeruli

Emre Yaksi and **Rachel I. Wilson**
Department of Neurobiology, Harvard Medical School, 220 Longwood Ave., Boston MA 02115

Abstract

In the *Drosophila* antennal lobe, excitation can spread between glomerular processing channels. In this study, we investigated the mechanism of lateral excitation. Dual recordings from excitatory local neurons (eLNs) and projection neurons (PNs) showed that eLN-to-PN synapses transmit both hyperpolarization and depolarization, are not diminished by blocking chemical neurotransmission, and are abolished by a gap junction mutation. This mutation eliminates odor-evoked lateral excitation in PNs and diminishes some PN odor responses. This implies that lateral excitation is mediated by electrical synapses from eLNs onto PNs. In addition, eLNs form synapses onto inhibitory LNs. Eliminating these synapses boosts some PN odor responses and reduces the disinhibitory effect of GABA receptor antagonists on PNs. Thus, eLNs have two opposing effects on PNs, driving both direct excitation and indirect inhibition. We propose that when stimuli are weak, lateral excitation promotes sensitivity, whereas when stimuli are strong, lateral excitation helps recruit inhibitory gain control.

INTRODUCTION

Sensory neurons are generally selective for particular stimulus features. Neurons at the same level of sensory processing that are tuned to different features can be thought of as representing different “processing channels” A fundamental question in sensory neuroscience is to understand the mechanisms and functions of cross-talk between such channels.

The notion of a sensory channel is particularly well-defined in early olfactory processing. This is because each glomerulus in the olfactory bulb or antennal lobe defines both an anatomical module and a discrete feedforward circuit. Each olfactory receptor neuron (ORN) is presynaptic to a single glomerulus, and each second-order neuron is postsynaptic to a single glomerulus (Bargmann, 2006). Functional connections between processing channels were until recently thought to be mainly inhibitory, with little or no spread of excitation between principal neurons in different glomeruli (but see Laurent et al., 2001; Lledo et al., 2005; Schoppa and Urban, 2003). Recently, however, several studies in the *Drosophila* antennal lobe demonstrated the existence of excitatory connections between second-order neurons in different glomeruli (Olsen et al., 2007; Root et al., 2007; Shang et al., 2007). These studies found that when the ORN inputs to a second-order neuron were silenced, that neuron still received indirect odor-evoked excitation from other glomeruli (which we define here as “lateral excitation”). These studies proposed that lateral excitation was mediated by local neurons (LNs) that extend dendrites into many glomeruli and form dendrodendritic synapses with second-order neurons (termed projection neurons, or PNs).

Correspondence to: Rachel I. Wilson, rachel_wilson@hms.harvard.edu.

Both the mechanism and function of lateral excitation are uncertain. It has been suggested that its function might be to boost responses to weak stimuli (Olsen et al., 2007; Shang et al., 2007), but this could not be directly tested because there was no known way to abolish lateral excitation. It was also proposed that lateral excitation is mediated by the release of acetylcholine from LNs (Shang et al., 2007). However, this could not be directly tested because cholinergic antagonists block the transmission of all olfactory signals to the brain; this is due to the fact that ORNs are themselves cholinergic (Kazama and Wilson, 2008). Moreover, lateral excitation is recruited very rapidly after ORN signals reach the brain, with a delay almost too short for a disynaptic connection (1.5 msec; Kazama and Wilson, 2008). This rapid recruitment of lateral excitation suggests that the underlying mechanism might be unusual.

In this study, we had two broad aims. Our first aim was to determine the synaptic mechanisms responsible for the spread of excitation between glomeruli. Our second aim was to discover how eliminating these mechanisms alters the output of the antennal lobe in response to olfactory stimuli.

RESULTS

Optogenetic stimulation of LNs produces mixed excitation/inhibition in PNs

When direct ORN input to a PN is silenced, olfactory stimuli can still elicit an excitatory response (Olsen et al., 2007; Root et al., 2007; Shang et al., 2007). This is thought to reflect the action of excitatory LNs (eLNs). However, it has not been directly demonstrated that any LNs actually have excitatory effects on other neurons. Several studies have noted the existence of GABA-immunonegative LNs (Chou et al., 2010; Shang et al., 2007; Wilson and Laurent, 2005) which are potential candidates for excitatory LNs. Among the Gal4 lines that reportedly drive expression in LNs, none is specific to GABA-negative LNs, but about half of the LNs labeled by *krasavietz-Gal4* are GABA-negative (58–61%; Chou et al., 2010; Shang et al., 2007), making it a useful starting point. Shang et. al. (2007) reported that GABA-negative *krasavietz* LNs are immunopositive for choline acetyltransferase (Cha), although a later study reported that not all are Cha-positive (Chou et al., 2010), casting some doubt on their function.

We therefore began by asking whether *krasavietz* LNs can excite PNs. We used *krasavietz-Gal4* to drive expression of both a GFP reporter and a light-activated cation channel (channelrhodopsin-2 or ChR2; Boyden et al., 2005). Targeted whole-cell *in vivo* recordings from GFP-labeled LNs confirmed that blue light depolarized these neurons and elicited a train of spikes (Figure 1A,B).

We then made whole-cell *in vivo* recordings from PNs in these flies. Optogenetic stimulation of *krasavietz* LNs evoked both excitation and inhibition in PNs (Figure 1C,D). If the PN response were due to the combined action of cholinergic and GABAergic LNs, it should be completely blocked by Cd^{2+}, a broad-spectrum antagonist of voltage-dependent calcium channels and thus a blocker of chemical synaptic transmission. However, in the presence of Cd^{2+} the excitatory component was actually increased, and only the inhibitory component was abolished (Figure 1D). Subtraction of the traces recorded before and after adding the drug revealed that the Cd^{2+}-sensitive component is hyperpolarizing and slow, whereas the Cd^{2+}-insensitive component is depolarizing and fast (Figure 1E). As a negative control, we also recorded from PNs in flies that lacked the *krasavietz-Gal4* driver. Light evoked almost no response, confirming that most of the PN response in flies harboring the *krasavietz-Gal4* driver was due to ChR2-mediated currents in Gal4-expressing cells (data not shown). Taken together, these results imply that the *krasavietz* population includes eLNs, but eLNs do not excite PNs through chemical synapses.

Identifying eLNs

As a next step, we aimed to locate the GABA-negative LNs within the *krasavietz* population. We labeled krasavietz LNs with CD8:GFP and performed dual immunofluorescence confocal microscopy using anti-GABA and anti-CD8 antibodies. We observed that GABA-negative *krasavietz* LN somata were located just ventro-lateral to the antennal lobe neuropil (Figure 2A). By comparison, most of the GABA-positive labeled somata were dorso-lateral to the antennal lobe, fewer located ventrally. This suggested that we could preferentially study eLNs by targeting the ventral region.

To test this idea, we performed dual whole-cell recordings from PNs and *krasavietz* LNs. We injected depolarizing current into each recorded LN to produce a depolarization and a train of spikes (Figure 2B,C). This could evoke either depolarization (Figure 2B) or hyperpolarization (Figure 2C) in the simultaneously-recorded PN. In some cases, there was no PN response. Consistent with the immunostaining results, we only observed depolarization in the PN when we were recording from LNs located in the ventral region. When we observed hyperpolarization in the PN, it was generally when we were recording from LNs located dorsally. In total, we performed 74 dual recordings from PNs and *krasavietz* LNs, of which 37 showed an excitatory LN-PN connection, 17 showed an inhibitory LN-PN connection, and the remainder showed no connection.

In these experiments, we also noticed that the LNs that depolarized PNs had distinctive electrophysiological properties. Specifically, these cells were always barraged by spontaneous inhibitory postsynaptic potentials (IPSPs; Figure 2D). In these cells we also typically saw small events resembling attenuated action potentials (~10 mV amplitude; Figure 2D) in addition to full-sized spikes (~40 mV amplitude). In our paired recordings, every LN that made made an excitatory connection with the simultaneously-recorded PN also had these distinctive electrophysiological properties. The converse was also true: every LN with these properties also made an excitatory connection with the PN, implying that each eLN is connected to most or all PNs. By contrast, we never saw these properties in LNs that hyperpolarized PNs (Figure 2E). In the experiments that follow, we use the presence of spontaneous IPSPs, together with soma location and GFP expression, as our diagnostic method of identifying eLNs.

Odor responses of eLNs can account for the properties of lateral excitation

If eLNs mediate lateral excitation, then they should be excited by odors. In addition, their odor selectivity should correlate with the selectivity of lateral excitation. In order to test these predictions, we made recordings from eLNs while presenting a chemically diverse panel of odors. We selected odors that would elicit a broad range of total activity levels in the ORN population (Hallem and Carlson, 2006). We verified this using local field potential recordings from the antenna, which provide a rough estimate of the total amount of ORN activity (Olsen et al., 2010). These recordings confirmed that this odor panel elicits a wide range of total ORN activity levels (Figure 3A,B).

Next, we recorded from eLNs to determine how they respond to odors. Interestingly, all the odors in our test panel elicited similar eLN responses, regardless of their chemical structure or the total amount of ORN activity they elicited (Figure 3C,D). Every eLN we recorded from was broadly tuned to odors and was sensitive to even weak ORN input. Finally, we asked how the responses of eLNs compare with the properties of lateral excitation. We removed the feedforward inputs to a subset of PNs by bilaterally removing the olfactory organ housing their cognate ORNs (either the antennae for PNs in an antennal glomerulus, or the palps for PNs in a palp glomerulus). We labeled deafferented PNs with GFP and recorded specifically from these cells while stimulating ORN input to other glomeruli using

our panel of test odors. Again, we observed that all the odors in the panel elicited similar lateral excitation in these PNs (Figure 3E,F). Qualitatively similar results were observed for PNs in three different glomeruli (VC1, VC2, DM1).

These results are consistent with the hypothesis that eLNs are the neural substrate of lateral excitation. The sensitivity and broad tuning of lateral excitation have been noted previously (Olsen et al., 2007; Shang et al., 2007). Our results imply that these properties reflect the odor response characteristics of eLNs themselves.

eLNs make electrical synapses onto PNs

In contrast to a previous study that proposed that eLNs excite PNs by releasing acetylcholine (Shang et al., 2007), our optogenetic stimulation experiments suggest that eLNs do not excite PNs through chemical synapses. However, because this technique activates a mixed population of LNs, the interpretation of this result is complicated by co-activating excitatory and inhibitory inputs. We therefore turned to dual intracellular recordings to examine the properties of eLN-PN connections in a more selective manner. We found that depolarizing the eLN elicited a depolarization in the PN, whereas hyperpolarizing the eLN elicited a hyperpolarization in the PN (Figure 4A,B). Blocking chemical synaptic transmission with Cd^{2+} did not weaken the PN responses (Figure 4B,C). Similarly, the nicotinic acetylcholine receptor antagonist mecamylamine had no effect, although two other nicotinic antagonists had weak effects in some experiments (Figure S1). It is difficult to determine whether there is a small chemical component to these synapses, and if so, whether this represents spillover or conventional synaptic transmission (see Discussion). What is clear is that eLNs are electrically coupled to PNs, and this represents the main mechanism by which eLNs depolarize PNs.

Two points are worth noting about the values of the coupling coefficients that we measured in these experiments (Figure 4C). First, although these coefficients are small, they almost certainly underestimate the strength of the connection at the synapse. This is because both electrodes are located at the soma, and the soma can be electronically distant from synaptic sites (Gouwens and Wilson, 2009). Thus, voltages will decay substantially while traveling from the presynaptic electrode to the synaptic site, and from the synaptic site to the postsynaptic electrode. Second, depolarizing signals were transmitted more effectively across this electrical connection than were hyperpolarizing signals (Figure 4B,C). This could reflect better propagation of depolarizing voltages to the site of the gap junction, and/or electrical rectification at the junction (Phelan et al., 2008).

Genetic elimination of synapses from eLNs onto PNs

We next asked whether we could genetically disrupt the connections from eLNs onto PNs. The *Drosophila* genome contains multiple genes coding for gap junction subunits (Phelan et al., 1998). Among these, *shaking-B* (*shakB*) is a good candidate. The *shakB* locus produces alternative transcripts, a set of which (*shakB.neural*) are expressed in the adult central nervous system (Sun and Wyman, 1996; Zhang et al., 1999). The $shakB^2$ allele produces a complete elimination of *shakB.neural* proteins. This mutation disrupts electrical connections in the optic lobe and in the giant fiber escape pathway (Curtin et al., 2002; Phelan et al., 1996; Sun and Wyman, 1996; Thomas and Wyman, 1984), and it produces defects in visual escape behaviors and increased seizure susceptibility (Kuebler and Tanouye, 2000; Thomas and Wyman, 1984).

We began by asking whether *shakB* is expressed by antennal lobe neurons. We used patch electrodes to collect the somata of individual GFP-labeled PNs, pooled these samples, and performed RT-PCR with nested primers designed to detect *shakB* transcripts. We detected a

clear band at the predicted size (Figure S2), meaning that this gap junction subunit is likely expressed in antennal lobe PNs.

We then tested whether the *shakB*^{2} mutation eliminates electrical synapses from eLNs onto PNs. Dual recordings showed that connections from eLNs onto PNs were completely abolished in mutant flies (Figure 4B–C). These results are consistent with the idea that eLN-to-PN synapses are electrical connections.

eLNs receive cholinergic excitation from PNs

Dual recordings also gave us the opportunity to examine synaptic transmission in the reverse direction, from PNs onto eLNs (Figure 4D). In every pair we recorded, stimulating the PN depolarized the eLN (Figure 4E). This implies that each eLN receives excitation from most or all PNs. PN-to-eLN synapses transmitted both depolarizing and hyperpolarizing signals (Figure 4E,F). Cd^{2+} had no effect on transmission of hyperpolarizing steps, but did significantly reduce transmission of depolarizing steps (Figure 4E,F). A nicotinic antagonist had a similar effect (Figure S1). These results imply that PN-to-eLN synapses are mixed chemical-electrical synapses. Consistent with this conclusion, we found that the *shakB*^{2} mutation abolishes the transmission of hyperpolarizing steps but not depolarizing steps (Figure 4E,F). Together, these results show that PNs release acetylcholine onto eLNs, in addition to coupling electrically to eLNs.

eLNs make mixed synapses onto iLNs

Our results suggest that eLNs do not release acetylcholine onto PNs. However, some GABA-negative *krasavietz* LNs are Cha-positive (Chou et al., 2010; Shang et al., 2007), implying that these cells do synthesize acetylcholine. This raises the question of whether eLNs release acetylcholine onto cells other than PNs. In particular, we wondered whether eLNs might make cholinergic synapses onto iLNs.

To investigate this, we performed dual recordings between eLNs and iLNs (Figure 5A). In many of these pairs, depolarizing the eLN produced a depolarizing response in the iLN (Figure 5B). This was substantially reduced by Cd^{2+} (Figure 5B,C) and by a nicotinic antagonist (Figure S1). This implies that eLN-to-iLN synapses are largely cholinergic, whereas eLN-to-PN synapses are mainly or purely electrical. (It is possible that some eLN-to-iLN connections are polysynaptic, but the fact that some of these connections were relatively strong makes it unlikely that they are all polysynaptic.)

These synapses also likely have an electrical component, because hyperpolarizing the eLN generally hyperpolarized the iLN (Figure 5B,C). We therefore tested whether the *shakB*^{2} mutation alters these connections. Surprisingly, connections from eLNs onto iLNs were completely gone in mutant flies (Figure 5B,C). This is unexpected because the chemical component of these connections should not necessarily depend on the electrical component. This result implies that the electrical component of this synapse is required for the proper development of the chemical component.

We also examined synaptic transmission in the reverse direction, from iLNs onto eLNs (Figure 5D). In some cases, we saw the signature of an electrical connection—namely, weak transmission of both depolarizing and hyperpolarizing pulses from the iLN to the eLN (Figure 5E). In other cases, depolarizing the iLN strongly hyperpolarized the eLN (Figure 5E), suggesting that iLNs can release GABA onto eLNs.

Together, these results demonstrate that excitatory and inhibitory LNs are interconnected. This in turn suggests that eLNs play a role in the recruitment of GABAergic inhibition.

PN-PN interactions require electrical synapses

These recordings revealed that *shakB* is required for the proper development of the chemical component of eLN-to-iLN synapses. Given this, we wondered whether *shakB* is also required for the chemical component of yet another chemical-electrical synapse—namely, the reciprocal synapse between PNs in the same glomerulus. This synapse transmits both depolarizing and hyperpolarizing steps, and the transmission of depolarizing steps is partially blocked by Cd^{2+} (Kazama and Wilson, 2009).

In order to record from pairs of such "sister" PNs simultaneously, we took advantage of a Gal4 line which labels seven PNs in glomerulus DA1 (Berdnik et al., 2006; Jefferis et al., 2004). We recorded from pairs of GFP-positive DA1 PNs and probed their reciprocal connections (Figure 6A). In control flies, we found that DA1 PNs were always reciprocally connected, and both depolarizing and hyperpolarizing steps were transmitted across these connections. In the *shakB*^{2} mutant, we found that these connections were completely abolished (Figure 6B,C).

We interpret this as evidence that sister PNs are normally coupled by mixed chemical-electrical connections, but that the electrical component is required for the proper development of the chemical component. Interestingly, this result has a direct precedent in the mouse olfactory bulb, where electrical synapses between sister mitral cells are required for the development of chemical synapses between these cells (Maher et al., 2009). We cannot exclude the idea that sister PNs couple indirectly by synapsing onto the same eLN, but this seems unlikely given that PN-PN interactions are relatively strong.

Genetic elimination of odor-evoked lateral excitation

We have shown that the *shakB*^{2} mutation eliminates eLN-to-PN synapses. Therefore, if eLNs mediate odor-evoked lateral excitation, then the *shakB*^{2} mutation should eliminate this phenomenon. To test this idea, we focused on PNs in three different glomeruli: VC1, VC2, and DM1. We labeled these PNs with GFP to target them specifically with our electrodes, and we removed their feedforward inputs by removing the olfactory organ housing their cognate ORNs. For example, VC1 ORNs are housed in the maxillary palp, and so we removed the palp when we recorded from these PNs so that we could observe purely lateral signals from antennal glomeruli. In this type of recording configuration, we found that all test odors elicited reliable lateral excitation in wild-type PNs, but no odors elicited any lateral excitation in *shakB*^{2} mutant PNs (Figure 6). This result supports the conclusion that eLNs mediate odor-evoked lateral excitation. (Note that in the mutant, weak odor-evoked lateral inhibition was observed; this is consistent with a previous report that there is a small amount of postsynaptic lateral inhibition in this circuit (Olsen and Wilson, 2008), although most lateral inhibition is presynaptic.)

For all three PN types we recorded from, the *shakB*^{2} mutation had the same effect, arguing that the mechanism of lateral excitation is not glomerulus-specific. This is an important result because different PNs can receive either strong or weak lateral excitation depending on the glomerulus they innervate (Olsen et al., 2007). In these experiments, we noticed that wild-type VC1 and VC2 PNs showed lateral excitation of a size that was typical of most other glomeruli (Olsen et al., 2007), whereas wild-type DM1 PNs consistently showed smaller lateral excitation (Figure 6). Because the *shakB*^{2} mutation abolishes lateral excitation in all three cases, we would interpret this heterogeneity as reflecting stronger electrical coupling with the eLN network in some glomeruli, and weaker coupling in other glomeruli.

As a control, we verified that expressing a *shakB.neural* transgene under Gal4/UAS control rescues odor-evoked lateral excitation (Figure S3). This result shows that the phenotype is

due to loss of *shakB*, and is not an artifact of the genetic background. We also performed a series of control experiments to verify the specificity of the mutant phenotype. First, we confirmed that PN morphology and glomerular compartmentalization is normal in the mutant (Figure S4). Then, we verified that ORN odor responses are also normal (Figure S4). Finally, we checked that iLN-PN connections are normal (Figure S4). Taken together, these results show that the antennal lobe is essentially normal in the *shakB*^{2} mutant, except for three types of synapses which have an electrical component and which are abolished: eLN-to-PN synapses, eLN-to-iLN synapses, and PN-PN reciprocal synapses.

Eliminating lateral excitation can reduce PN odor responses

Given that the *shakB*^{2} mutation eliminates three specific types of synapses in the antennal lobe, we then asked whether this mutation alters PN spiking responses to odors in an otherwise intact circuit. Because *shakB*^{2} eliminates synapses from eLNs onto PNs, we might predict that it reduces some PN odor responses. Furthermore, *shakB*^{2} also eliminates PN-PN reciprocal synapses, and this is another reason why we would predict that it reduces some PN odor responses. However, because this mutation also eliminates eLN-to-iLN synapses, it might reduce the recruitment of inhibition, and so we might predict that it actually increases some PN odor responses.

To investigate this, we compared PN odor responses in control flies and *shakB*^{2} mutants. We used GFP labeling to target our electrodes to PNs in four glomeruli: VC1, DA1, VC2, and DM1. We exploited differences in the way these four types of PNs couple to other glomeruli and to sister PNs in order to disambiguate changes in lateral excitation, lateral inhibition, and PN-PN synapses.

We began with glomerulus VC1 (Figure 8A) because only one PN is known to be present in this glomerulus (Tanaka et al., 2004; see also Experimental Procedures). If only one PN is present, this would simplify the situation because it would mean that there are no PN-PN synapses. In VC1 PNs, we found that responses to all the test odors were weaker in *shakB*^{2} flies as compared to controls, and for many odors, this difference was statistically significant (Figure 8B,C).

If this phenotype reflects a loss of lateral excitation, it should disappear for a stimulus which is specific to VC1 ORNs. Fortunately, these ORNs are the only neurons in the palp that respond to the odor fenchone (Goldman et al., 2005). Some antennal ORNs also respond to this odor (data not shown), but we made fenchone a “private” odor for VC1 by removing the antennae. When we recorded from VC1 PNs in flies with intact antennae, fenchone elicited an excitatory response which was significantly smaller in *shakB*^{2} mutant flies (Figure 8A,B), implying that this odor elicits lateral excitation onto VC1 from antennal glomeruli. By contrast, when we recorded from VC1 PNs in flies with antennae removed, there was no difference between control and *shakB*^{2} responses (Figure 8D,E). This supports the idea that the phenotype is due to the loss of lateral excitation, at least for this PN and these odors.

Eliminating PN-PN interactions can reduce PN odor responses

Next, we examined a second glomerulus, DA1. This glomerulus is notable for containing an unusually large number of sister PNs (seven in total; Berdnik et al., 2006). The only known ligand for DA1 ORNs is cis-vaccenyl acetate, which is also relatively selective for these ORNs (Clyne et al., 1997; Schlief and Wilson, 2007; van der Goes van Naters and Carlson, 2007). Thus, cis-vaccenyl acetate should elicit reciprocal excitation among sister DA1 PNs, but little or no lateral input to these PNs, providing us with an opportunity to look specifically at the role of sister PN interactions in shaping PN odor responses.

We confirmed that cis-vaccenyl acetate elicits an excitatory response in DA1 PNs (Figure 8F,G), as previously reported (Schlief and Wilson, 2007). In *shakB*^{2} mutant flies, we found that this response was significantly smaller than in control flies (Figure 8G). Because *shakB*^{2} eliminates reciprocal synapses between DA1 PNs (Figure 6), and because cis-vaccenyl acetate is a relatively "private" odor for DA1 ORNs, this result implies that PN-PN synapses can amplify odor responses.

Perturbing electrical networks can increase PN odor responses by reducing inhibition

We next turned to glomerulus VC2. In this glomerulus, as in VC1, only one PN may be present (Tanaka et al., 2004). As in VC1, we found that some VC2 PN spiking responses to odors were significantly diminished in the *shakB*^{2} mutant (Figure 9A–C). However, other responses were significantly larger in the mutant (Figure 9B,C). Given that this mutation eliminates eLN-to-iLN synapses, this phenotype might reflect a defect in the recruitment of GABAergic inhibition. To test this, we compared the effect of adding GABA receptor antagonists (5 μM picrotoxin and 20 μM CGP54626) in control versus mutant PNs. If *shakB*^{2} reduces the amount of GABAergic inhibition recruited by these stimuli in VC2 PNs, then the antagonists should have a smaller effect on mutant VC2 PN odor responses. Indeed, we found that the disinhibitory effect of adding the antagonists was significantly smaller in the mutant than in controls (Figure 9D,E). This is consistent with the conclusion that eLNs are involved in recruiting GABAergic inhibition, presumably via their excitatory synapses onto iLNs.

Finally, we also examined glomerulus DM1. As in VC1 and VC2, only one PN is known to reside in this glomerulus. Unlike VC1 and VC2 PNs, DM1 PNs receive only weak lateral excitation, suggesting weak coupling to the eLN network (Figure 7). Perhaps not surprisingly, the *shakB*^{2} mutation had no significant effect on DM1 PN odor responses (Figure S5). This negative result is consistent with our conclusion that the gross anatomy of the antennal lobe is normal in *shakB*^{2} mutants, as are ORN odor responses (Figure S4).

DISCUSSION

Target-cell-specific properties of eLN synapses

Our findings directly demonstrate that LNs can excite PNs. Putative excitatory local neurons have been identified in the olfactory bulb (Aungst et al., 2003), but they have not been shown to have excitatory effects on principal neurons. In this study, we show directly for the first time that local neurons can excite principal neurons and thereby spread activity between glomeruli.

A previous study proposed that excitatory LNs depolarize PNs by releasing acetylcholine (Shang et al., 2007), based on the finding that some *krasavietz* LNs are immunopositive for Cha. However, using an optogenetic approach, we find that selectively stimulating *krasavietz* eLNs produces an excitatory response which is insensitive to blocking synaptic vesicle exocytosis, suggesting primarily electrical rather than chemical coupling from eLNs onto PNs. Moreover, dozens of dual recordings from *krasavietz* eLNs and PNs revealed clear evidence of electrical connections. Together, these results are strong evidence that *krasavietz* LNs couple to PNs electrically. We found it was difficult to determine conclusively whether eLN-to-PN synapses have a small cholinergic component. On one hand, we found that, on average, neither Cd^{2+} nor mecamylamine nor D-tubocurarine had any effect, and this argues against a cholinergic component. On the other hand, α-bungarotoxin slightly inhibited coupling (Figure S1). In any event, it is clear that this synapse is largely (if not purely) electrical.

Given these results, it is interesting that eLNs synapses onto iLNs clearly have a strong chemical component. Unlike eLN-to-PN synapses, eLN-to-iLN synapses were almost completely blocked by either Cd^{2+} or mecamylamine (Figure S1). This implies that the properties of eLN output synapses are target-cell specific: synapses onto PNs are largely or purely electrical, whereas synapses onto iLNs are largely chemical with a smaller electrical component. There are several examples in the literature of a neuron forming synapses with different properties onto different types of target cells (Pelkey and McBain, 2007), but this example of target-cell specialization seems particularly striking.

Functional implications of electrical synapses

What is the functional relevance of our finding that eLNs form electrical synapses onto PNs? One distinctive property of electrical connections is their speed. This helps explain why lateral excitation is recruited so rapidly. Indeed, electrical stimulation of the antennal nerve elicits depolarization in maxillary palp glomeruli only about 1.5 msec after onset of depolarization in an antennal glomerulus (Kazama and Wilson, 2008). This suggests that the eLN network contributes to the earliest time points in the PN odor response. Consistent with this idea, we often saw differences between control and *shakB*^{2} mutant PNs during the earliest epoch of PN responses (e.g., Figure 8B). Thus, lateral excitation may be preferentially involved in the rising phase of PN odor responses, whereas inhibition seems to be recruited more slowly (Figure 1E). Preferential transmission of the rising phase of an odor pulse may speed odor detection and promote resolution of odor rapid fluctuations (Bhandawat et al., 2007).

Another characteristic feature of electrical synapses is that they are less noisy than chemical synapses (Connors and Long, 2004). A previous study showed that whereas noise in sister PNs is highly correlated, noise is almost entirely uncorrelated in PNs innervating different glomeruli (Kazama and Wilson, 2009). That result implied that LNs contribute relatively little correlated noise to PNs. Our finding that eLN-PN connections are electrical rather than chemical may help explain why that is so. It also suggests that the eLN network is unlikely to add substantial noise to PN odor responses, contrary to a previous suggestion that this is the major function of eLNs (Shang et al., 2007).

A further characteristic property of electrical connections is that they can alter the way signals propagate through a cell. This is because an electrical connection acts as a shunt which diminishes the effect of a synaptic current on a cell's membrane potential. Thus, eliminating electrical connections can make neurons more electrotonically compact (Bennett and Zukin, 2004). Indeed, we observed that the *shakB*^{2} mutation significantly increased PN input resistance in PNs that normally receive relatively strong lateral excitation ($p<0.05$ for VC1 and VC2, Mann-Whitney U-tests; not significant in DA1 and DM1). This might be expected to increase PN responses to their direct ORN inputs, but this is not what we observed: when VC1 PNs were disconnected from lateral input (by removing the antennae), the *shakB*^{2} mutation did not increase the spiking responses of these PNs to their direct ORN inputs, despite the fact that PN input resistance was increased. The change in PN input resistance may be too small to have an effect on PN spike rate; alternatively, changes in PN input resistance may trigger compensatory changes in the strength of ORN-to-PN synapses, as has been shown previously (Kazama and Wilson, 2008).

Properties and functions of odor-evoked lateral excitation

Previous studies have noted two curious features of odor-evoked lateral excitation in the antennal lobe. First, even weak levels of ORN activity are sufficient to recruit lateral excitation onto PNs. Second, odor stimuli that differ in chemical structure and/or

concentration elicit somewhat similar levels of lateral excitation (Olsen et al., 2007; Shang et al., 2007).

Our results imply that these features reflect properties of eLNs themselves. Namely, eLNs respond robustly to even weak levels of ORN activity, and they are relatively indiscriminate in their responses. Each eLN extends its neurites into most or all glomeruli (data not shown), and so it may pool excitatory input from most or all glomeruli. Moreover, we found that the probability of finding a connection from a randomly-chosen PN onto an eLN was 100%. This suggests that all PNs converge onto each eLN. If so, this would help explain why eLNs are sensitive to even weak odors and are excited by all chemical classes of odors.

What is the function of spreading excitation between glomeruli? We suggest that eLNs may function to slightly and transiently increase the excitability of all PNs when any ORN channel is activated. In addition, eLNs might have a role in promoting synchrony among PN spikes. As a result, the eLN network could improve odor detection when stimuli are weak. An obvious potential problem with this network is that spreading excitation between glomeruli could destroy PN odor selectivity. However, this is evidently not a problem in practice because PNs are in fact odor selective (Bhandawat et al., 2007). In this study, we found that increasing level of ORN activity does not substantially increase the strength of eLN odor responses. This ceiling on eLN activity might be useful in preventing lateral excitation from becoming too powerful when odors are strong. In other words, the tendency for eLN odor responses to saturate should help preserve PN odor selectivity.

Interactions among LNs

Thus far, thinking about the functional relevance of eLNs has considered only their role in connecting PNs in different glomeruli. In this study, we discovered that eLNs provide excitatory input not only to PNs, but also to iLNs. Indeed, eLN synapses onto iLNs are stronger than their synapses onto PNs. This implies that a major function of eLNs is to recruit GABAergic inhibition.

Consistent with this, we found that some PN odor responses are actually potentiated by the *shakB*^{2} mutation, which suggests a loss of inhibition which is large enough to outweigh the loss of lateral excitation. Moreover, whereas in control flies some odor responses were substantially disinhibited by GABA receptor antagonists, in *shakB*^{2} flies these responses were much less disinhibited when GABA receptors were blocked. This result supports the idea that eLNs provide an important source of excitatory drive to iLNs, although iLNs also receive excitatory input from PNs (Figure S4; see also Wilson et al., 2004).

The idea that interneurons can excite other interneurons—thereby modulating inhibition of principal cells—has a precedent in other neural circuits. For example, the vertebrate retina contains two layers of electrically-coupled inhibitory interneurons: horizontal cells in the outer retina, and amacrine cells in the inner retina. Because these retinal networks are purely electrical, they are not thought to boost the overall level excitation in the interneuron network; rather, they are thought to simply average signals across neighboring cells, thus creating a more uniform inhibitory surround (Bloomfield and Volgyi, 2009). In the antennal lobe, electrical coupling between eLNs and iLNs may serve an analogous “smoothing” function. But because eLNs also excite iLNs through chemical synapses, eLNs are likely to also boost the overall level of excitation in iLNs, thereby boosting inhibition of PNs.

Why might it be useful for eLNs to drive both direct excitation of PNs and indirect inhibition of PNs? We propose that the relative importance of these two effects depends on odor intensity. The excitatory drive relayed by eLNs onto PNs is probably most important when odor stimuli are weak. When stimuli are strong, the excitation that eLNs provide to

iLNs may be relatively more important. Although we found that increasing stimulus intensity does not substantially increase eLN activity, PN input to iLNs is likely growing as ORN activity rises. It may be the combined excitatory drive from eLNs and PNs onto iLNs that causes GABAergic inhibition to grow with rising ORN activity (Olsen et al., 2010; Olsen and Wilson, 2008). Increasing inhibition helps prevent PN activity from saturating, and may promote odor discrimination (Asahina et al., 2009; Olsen et al., 2010; Root et al., 2008; Sachse and Galizia, 2003).

A challenge for understanding neural circuits

Electrical networks are pervasive in both vertebrates and invertebrates (Bennett and Zukin, 2004; Connors and Long, 2004; Phelan, 2005). Thus, understanding signal propagation in electrical networks has fundamental importance for understanding how neural circuits function. Several new genetic approaches to control neural circuits *in vivo* involve disrupting synaptic vesicle release (Luo et al., 2008; Simpson, 2009). However, electrical synapses will be unaffected by these perturbations. Other approaches involve introducing channels that are controlled by light or unnatural ligands (Luo et al., 2008; Simpson, 2009). However, the effects of opening a channel in specific cell populations can differ for electrical versus chemical networks, because electrical connections are bidirectional whereas chemical connections are not. These considerations should inspire caution in interpreting experiments using these approaches, and also emphasize the need for new tools to specifically perturb electrical networks.

EXPERIMENTAL PROCEDURES

Fly stocks

Flies were raised at 25°C on conventional cornmeal agar medium under a 12/12 hour light/dark cycle. All experiments were performed on adult female flies, 1–3 days post-eclosion (except where otherwise noted). Gal4 lines were previously described as follows: *krasavietz-Gal4* on chromosome 3 (drives Gal4 expression in both GABA+ LNs and GABA- LNs; Chou et al., 2010; drives Gal4 expression in both GABA+ LNs and GABA- LNs; Shang et al., 2007); *GH146-Gal4* on chromosome 2 (drives Gal4 expression in a large fraction of PNs; Stocker et al., 1997); *NP5221-Gal4* on chromosome 2 (drives Gal4 expression in 1 VC1 PN, 1 VC2 PN, and 1 DM1 PN; Tanaka et al., 2004); *Mz19-Gal4* on chromosome 2 (drives Gal4 expression in 7 DA1 PNs; Berdnik et al., 2006; drives Gal4 expression in 7 DA1 PNs; Jefferis et al., 2004). The *krasavietz-Gal4* line drives Gal4 expression in at least three eLNs per antennal lobe, based on the fact that we have recorded sequentially from three GFP-positive eLNs in the same antennal lobe when GFP was expressed under the control of this driver. While we assume that the *NP5221-Gal4* line drives Gal4 expression all the PNs in glomeruli VC1, VC2, and DM1 (i.e., 1 PN in each of these three glomeruli), we cannot exclude the idea that there are other PNs in these three glomeruli that do not express Gal4. However, in experiments where we labeled PNs in specific glomeruli with photo-activatible GFP (expressed under the Cha promoter), we have found that the total number of PNs in most individual glomeruli is generally the same as the number labeled by enhancer-trap Gal4 lines in our laboratory (W.W. Liu and R.I. Wilson, unpublished observations), so we think this assumption is reasonable. Lines with UAS-linked transgenes were previously described as follows: *UAS-CD8:GFP* on chromosomes 2 and 3 (Lee and Luo, 1999); *UAS-ChR2:YFP* on chromosomes 2 and 3 (Hwang et al., 2007; lines “C” and “B”); *UAS-shakB.neural* on chromosome 2 (Curtin et al., 2002). The $shakB^{2}$ mutation has been previously characterized (Baird et al., 1990; Homyk et al., 1980).

Electrophysiology

*In vivo w*hole cell patch clamp recordings from the somata of PNs and LNs were performed as described previously (Wilson and Laurent, 2005). The external saline solution bathing the brain contained (in mM): 103 NaCl, 3 KCl, 5 *N*-Tris(hydroxymethyl)methyl-2-aminoethane-sulfonic acid, 8 trehalose, 10 glucose, 26 NaHCO3, 1 NaH2PO4, 1.5 CaCl2, and 4 MgCl2 (osmolarity adjusted to 270–275 mOsm). The saline was bubbled with 95% O_2/5% CO_2 and the pH equilibrated at 7.3. Patch-clamp electrodes were filled with an internal solution consisting of the following (in mM): 140 potassium aspartate, 10 HEPES, 1 EGTA, 4 MgATP, 0.5 Na_3GTP, 1 KCl, and 13 biocytin hydrazide. The pH of the internal solution was adjusted to 7.3 and the osmolarity was adjusted to ~ 265 mOsm. Local field potential recordings in the antenna (Figure 3) and single-sensillum recordings of ORN spikes (Figure S4) were performed essentially as described previously (Bhandawat et al., 2007; Olsen et al., 2007). Recordings were performed in current clamp mode using an Axopatch 200B amplifier (Axon Instruments). Recorded voltages were low-pass filtered at 2 kHz and digitized at 10 kHz. Data acquisition and all the analyses were performed in MATLAB (MathWorks) using custom software. All antagonists were prepared as concentrated stock solutions in water and then added to the saline perfusate to achieve the stated final concentration.

Immunohistochemistry

Identified PNs were filled with biocytin during the recording, and the morphology of the recorded neurons were visualized *post hoc* after fixation and after incubation with 1:1000 streptavidin:Alexa Fluor 568 (Invitrogen), as described previously (Bhandawat et al., 2007). The antennal lobe neuropil was visualized with a primary incubation of 1:10 mouse anti-nc82 antibody (Developmental Studies Hybridoma Bank, University of Iowa, Iowa City, IA) and a secondary incubation of 1:250 anti-mouse:Alexa Fluor 633 (Invitrogen), as described previously (Bhandawat et al., 2007). Images were acquired on a Zeiss LSM 510 confocal microscope with a 40× oil-immersion objective.

Olfactory stimulation

Odors were diluted in paraffin oil at the concentrations specified, except 4-methylphenol which was diluted in water. Dilutions were freshly prepared every 5 days. Details on the odor sources are posted at http://wilson.med.harvard.edu/odors.html. Odors were delivered with a custom-built olfactometer as described previously (Bhandawat et al., 2007) that dilutes the headspace of the odor vial a further ~10-fold in clean air before it reaches the fly. The flow rate of the odor delivery stream was 2.2 L/min. Odor stimuli were applied for 500 msec every 45 sec for 6 trials per odor per cell.

Optogenetic stimulation

Newly eclosed flies were cultured for 2 days in the dark on conventional medium supplemented with potato flakes rehydrated in an aqueous solution of all-trans-retinal. All-trans-retinal was prepared as a stock solution in ethanol (35 mM) and diluted 20-fold in water just before mixing with the potato flakes. Blue light was delivered using a 100-W Hg arc lamp (Olympus) attenuated with a 25% neutral density filter. Pulses of light (500 msec) were delivered every 5 sec using a shutter (Uniblitz) controlled by a TTL pulse. As a negative control, we recorded from PNs in flies lacking the Gal4 driver (genotype *UAS-Chr2:YFP; UAS-ChR2:YFP*) and confirmed that light elicited only a very small depolarization in these PNs (mean ± SEM = 0.2 ± 0.2 mV, n=5).

Dual whole-cell recordings

In the dual recordings involving eLNs, we expressed GFP under the control of the *krasavietz* Gal4 line to label eLNs, and we recorded from randomly-selected PNs or iLNs. Although PNs were not GFP-labeled in these recordings, they are identifiable based on their small-amplitude action potentials (Wilson et al., 2004; <12 mV). Cells identified as PNs in this way always formed excitatory connections onto eLNs. Similarly, although iLNs were not GFP-labeled in these experiments, they are identifiable based on their large-amplitude action potentials (Wilson et al., 2004; >25 mV) and lack of IPSPs (which distinguishes them from eLNs; see Figure 2). Cells identified as iLNs in this way never formed excitatory chemical synaptic connections onto other cells, but sometimes formed inhibitory chemical synaptic connections onto other cells which were blocked by GABA receptor antagonists (data not shown). In all dual recording experiments, the antennae were removed just before the experiment in order to minimize spontaneous activity. The intensity of current injection was adjusted in each experiment to achieve voltage deflections of approximately ± 40 mV in the cell into which current was injected. Current injections (500 msec duration) were repeated every 5 sec for 40–50 trials. The response of the unstimulated cell was low-pass filtered (50 Hz cutoff) to remove any spikes, and was averaged over all trials. The coupling coefficient was computed as the average change in membrane potential of postsynaptic neuron divided by that of the presynaptic neuron.

Data analysis

Spikes were detected using custom software. The coupling coefficient was calculated by dividing the trial-averaged membrane potential change in the postsynaptic cell by the change in the presynaptic cell. Peri-stimulus time histograms were generated by calculating the firing rate in 50-msec bins that overlapped by 25 msec. Mean PN spiking responses were quantified as the average spike rate during a 500-msec window beginning 100 msec after nominal stimulus onset, averaged across all 6 trials with a given stimulus (Figures 8 and 9). Lateral excitation in PNs was calculated as the average odor-evoked change in membrane potential (versus the pre-odor baseline membrane potential in each trial) during a 200-msec time window beginning 100 msec after nominal stimulus onset, averaged across all 6 trials (Figure 7 and Figure S3). All error bars/bands represent ± SEM values.

Supplementary Material

Refer to Web version on PubMed Central for supplementary material.

Acknowledgments

We are grateful to L.C. Griffith, K. Ito, L. Luo, G. Miesenböck, M.A. Tanouye, W.D. Tracey, and R.J. Wyman for gifts of fly stocks. D. Schmucker, N. Obholzer, and N. Jurish-Yaksi provided advice on RT-PCR experiments, and K.I. Nagel helped with the writing of the data acquisition software. We thank members of the Wilson lab for their feedback on the manuscript. This work was funded by a long-term fellowship from the Human Frontiers Science Program (to E.Y.), a grant from the NIH (R01DC008174), a McKnight Scholar Award, and Beckman Young Investigator Award (to R.I.W.). R.I.W. is an HHMI Early Career Scientist.

References

Asahina K, Louis M, Piccinotti S, Vosshall LB. A circuit supporting concentration-invariant odor perception in Drosophila. J Biol. 2009; 8:9. [PubMed: 19171076]

Aungst JL, Heyward PM, Puche AC, Karnup SV, Hayar A, Szabo G, Shipley MT. Centre-surround inhibition among olfactory bulb glomeruli. Nature. 2003; 426:623–629. [PubMed: 14668854]

Baird DH, Schalet AP, Wyman RJ. The Passover locus in Drosophila melanogaster: complex complementation and different effects on the giant fiber neural pathway. Genetics. 1990; 126:1045–1059. [PubMed: 2127576]

Bargmann CI. Comparative chemosensation from receptors to ecology. Nature. 2006; 444:295–301. [PubMed: 17108953]

Bennett MV, Zukin RS. Electrical coupling and neuronal synchronization in the Mammalian brain. Neuron. 2004; 41:495–511. [PubMed: 14980200]

Berdnik D, Chihara T, Couto A, Luo L. Wiring stability of the adult Drosophila olfactory circuit after lesion. J Neurosci. 2006; 26:3367–3376. [PubMed: 16571743]

Bhandawat V, Olsen SR, Schlief ML, Gouwens NW, Wilson RI. Sensory processing in the Drosophila antennal lobe increases the reliability and separability of ensemble odor representations. Nat Neurosci. 2007; 10:1474–1482. [PubMed: 17922008]

Bloomfield SA, Volgyi B. The diverse functional roles and regulation of neuronal gap junctions in the retina. Nat Rev Neurosci. 2009; 10:495–506. [PubMed: 19491906]

Boyden ES, Zhang F, Bamberg E, Nagel G, Deisseroth K. Millisecond-timescale, genetically targeted optical control of neural activity. Nat Neurosci. 2005; 8:1263–1268. [PubMed: 16116447]

Chou YH, Spletter ML, Yaksi E, Leong JC, Wilson RI, Luo L. Diversity and wiring variability of olfactory local interneurons in the Drosophila antennal lobe. Nat Neurosci. 2010 advance online publication. 10.1038/nn.2489

Clyne P, Grant A, O'Connell R, Carlson JR. Odorant response of individual sensilla on the Drosophila antenna. Invert Neurosci. 1997; 3:127–135. [PubMed: 9783438]

Connors BW, Long MA. Electrical synapses in the mammalian brain. Annu Rev Neurosci. 2004; 27:393–418. [PubMed: 15217338]

Curtin KD, Zhang Z, Wyman RJ. Gap junction proteins expressed during development are required for adult neural function in the Drosophila optic lamina. J Neurosci. 2002; 22:7088–7096. [PubMed: 12177205]

Goldman AL, van der Goes van Naters W, Lessing D, Warr CG, Carlson JR. Coexpression of two functional odor receptors in one neuron. Neuron. 2005; 45:661–666. [PubMed: 15748842]

Gouwens NW, Wilson RI. Signal propagation in Drosophila central neurons. J Neurosci. 2009; 29:6239–6249. [PubMed: 19439602]

Hallem EA, Carlson JR. Coding of odors by a receptor repertoire. Cell. 2006; 125:143–160. [PubMed: 16615896]

Homyk T Jr, Szidonya J, Suzuki DT. Behavioral mutants of Drosophila melanogaster. III. Isolation and mapping of mutations by direct visual observations of behavioral phenotypes. Mol Gen Genet. 1980; 177:553–565. [PubMed: 6770227]

Hwang RY, Zhong L, Xu Y, Johnson T, Zhang F, Deisseroth K, Tracey WD. Nociceptive neurons protect Drosophila larvae from parasitoid wasps. Curr Biol. 2007; 17:2105–2116. [PubMed: 18060782]

Jefferis GS, Vyas RM, Berdnik D, Ramaekers A, Stocker RF, Tanaka NK, Ito K, Luo L. Developmental origin of wiring specificity in the olfactory system of Drosophila. Development. 2004; 131:117–130. [PubMed: 14645123]

Kazama H, Wilson RI. Homeostatic matching and nonlinear amplification at genetically-identified central synapses. Neuron. 2008; 58:401–413. [PubMed: 18466750]

Kazama H, Wilson RI. Origins of correlated activity in an olfactory circuit. Nat Neurosci. 2009; 12:1136–1144. [PubMed: 19684589]

Kuebler D, Tanouye MA. Modifications of seizure susceptibility in Drosophila. J Neurophysiol. 2000; 83:998–1009. [PubMed: 10669511]

Laurent G, Stopfer M, Friedrich RW, Rabinovich MI, Volkovskii A, Abarbanel HD. Odor encoding as an active, dynamical process: experiments, computation, and theory. Annu Rev Neurosci. 2001; 24:263–297. [PubMed: 11283312]

Lee T, Luo L. Mosaic analysis with a repressible cell marker for studies of gene function in neuronal morphogenesis. Neuron. 1999; 22:451–461. [PubMed: 10197526]

Lledo PM, Gheusi G, Vincent JD. Information processing in the mammalian olfactory system. Physiol Rev. 2005; 85:281–317. [PubMed: 15618482]

Luo L, Callaway EM, Svoboda K. Genetic dissection of neural circuits. Neuron. 2008; 57:634–660. [PubMed: 18341986]

Maher BJ, McGinley MJ, Westbrook GL. Experience-dependent maturation of the glomerular microcircuit. Proc Natl Acad Sci U S A. 2009; 106:16865–16870. [PubMed: 19805387]

Olsen SR, Bhandawat V, Wilson RI. Excitatory interactions between olfactory processing channels in the Drosophila antennal lobe. Neuron. 2007; 54:89–103. [PubMed: 17408580]

Olsen SR, Bhandawat V, Wilson RI. Divisive normalization in olfactory population codes. Neuron. 2010 in press.

Olsen SR, Wilson RI. Lateral presynaptic inhibition mediates gain control in an olfactory circuit. Nature. 2008; 452:956–960. [PubMed: 18344978]

Pelkey KA, McBain CJ. Differential regulation at functionally divergent release sites along a common axon. Curr Opin Neurobiol. 2007; 17:366–373. [PubMed: 17493799]

Phelan P. Innexins: members of an evolutionarily conserved family of gap-junction proteins. Biochim Biophys Acta. 2005; 1711:225–245. [PubMed: 15921654]

Phelan P, Bacon JP, Davies JA, Stebbings LA, Todman MG, Avery L, Baines RA, Barnes TM, Ford C, Hekimi S, et al. Innexins: a family of invertebrate gap-junction proteins. Trends Genet. 1998; 14:348–349. [PubMed: 9769729]

Phelan P, Goulding LA, Tam JL, Allen MJ, Dawber RJ, Davies JA, Bacon JP. Molecular mechanism of rectification at identified electrical synapses in the Drosophila giant fiber system. Curr Biol. 2008; 18:1955–1960. [PubMed: 19084406]

Phelan P, Nakagawa M, Wilkin MB, Moffat KG, O'Kane CJ, Davies JA, Bacon JP. Mutations in shaking-B prevent electrical synapse formation in the Drosophila giant fiber system. J Neurosci. 1996; 16:1101–1113. [PubMed: 8558239]

Root CM, Masuyama K, Green DS, Enell LE, Nassel DR, Lee CH, Wang JW. A presynaptic gain control mechanism fine-tunes olfactory behavior. Neuron. 2008; 59:311–321. [PubMed: 18667158]

Root CM, Semmelhack JL, Wong AM, Flores J, Wang JW. Propagation of olfactory information in Drosophila. Proc Natl Acad Sci U S A. 2007; 104:11826–11831. [PubMed: 17596338]

Sachse S, Galizia CG. The coding of odour-intensity in the honeybee antennal lobe: local computation optimizes odour representation. Eur J Neurosci. 2003; 18:2119–2132. [PubMed: 14622173]

Schlief ML, Wilson RI. Olfactory processing and behavior downstream from highly selective receptor neurons. Nat Neurosci. 2007; 10:623–630. [PubMed: 17417635]

Schoppa NE, Urban NN. Dendritic processing within olfactory bulb circuits. Trends Neurosci. 2003; 26:501–506. [PubMed: 12948662]

Shang Y, Claridge-Chang A, Sjulson L, Pypaert M, Miesenbock G. Excitatory local circuits and their implications for olfactory processing in the fly antennal lobe. Cell. 2007; 128:601–612. [PubMed: 17289577]

Simpson JH. Mapping and manipulating neural circuits in the fly brain. Adv Genet. 2009; 65:79–143. [PubMed: 19615532]

Stocker RF, Heimbeck G, Gendre N, de Belle JS. Neuroblast ablation in Drosophila P[GAL4] lines reveals origins of olfactory interneurons. J Neurobiol. 1997; 32:443–456. [PubMed: 9110257]

Sun YA, Wyman RJ. Passover eliminates gap junctional communication between neurons of the giant fiber system in Drosophila. off J Neurobiol. 1996; 30:340–348.

Tanaka NK, Awasaki T, Shimada T, Ito K. Integration of chemosensory pathways in the Drosophila second-order olfactory centers. Curr Biol. 2004; 14:449–457. [PubMed: 15043809]

Thomas JB, Wyman RJ. Mutations altering synaptic connectivity between identified neurons in Drosophila. J Neurosci. 1984; 4:530–538. [PubMed: 6699687]

van der Goes van Naters W, Carlson JR. Receptors and neurons for fly odors in Drosophila. Curr Biol. 2007; 17:606–612. [PubMed: 17363256]

Wilson RI, Laurent G. Role of GABAergic inhibition in shaping odor-evoked spatiotemporal patterns in the Drosophila antennal lobe. J Neurosci. 2005; 25:9069–9079. [PubMed: 16207866]

Wilson RI, Turner GC, Laurent G. Transformation of olfactory representations in the Drosophila antennal lobe. Science. 2004; 303:366–370. [PubMed: 14684826]

Zhang Z, Curtin KD, Sun YA, Wyman RJ. Nested transcripts of gap junction gene have distinct expression patterns. J Neurobiol. 1999; 40:288–301. [PubMed: 10440730]

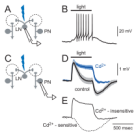

Figure 1. Optogenetic stimulation of LNs produces mixed excitation/inhibition in PNs

A. Activity in an LN that expresses channelrhodopsin is recorded with a whole-cell electrode at the soma in current-clamp mode. Genotype is *UAS-ChR2:YFP/+; krasavietz-Gal4,UAS-CD8:GFP/UAS-ChR2:YFP*.

B. Blue light depolarizes the LN and evokes a train of spikes.

C. Recording from a PN while exciting LNs.

D. Exciting LNs evokes mixed excitation-inhibition in PNs. Blocking chemical synaptic transmission with Cd^{2+} (100 μM) converts this to a purely excitatory response. Traces are averages across cells, ± SEM (*n*=5).

E. Subtracted traces show that Cd^{2+}-insensitive transmission consists of fast excitation, whereas Cd^{2+}-sensitive transmission consists of slow inhibition.

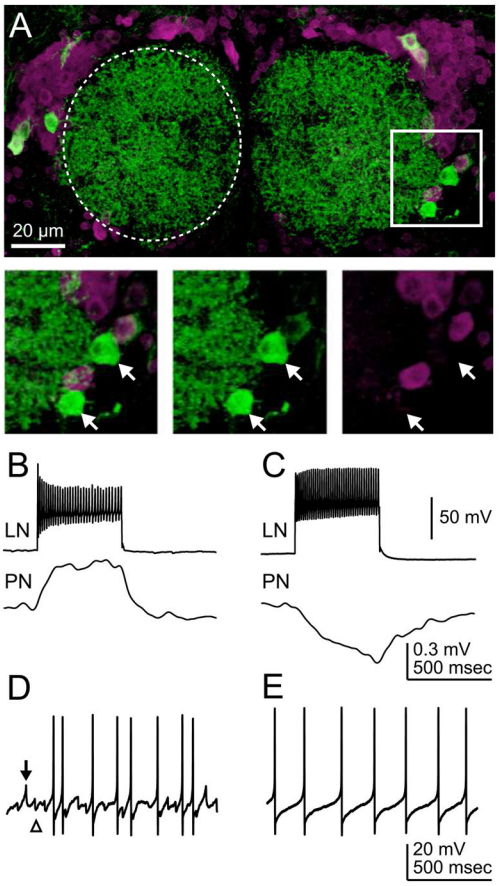

Figure 2. Identifying excitatory LNs

A. Projection of a confocal *z*-stack through a portion of the antennal lobes. Dorsal is up. CD8:GFP (green) labels *krasavietz* LNs, and anti-GABA immunofluorescence (magenta) labels GABAergic neurons. LN dendrites fill each antennal lobe (dotted circle). Inset (square) shows that some ventrolateral LN somata are GABA-negative. Other LN somata are located outside these sections. Genotype is *krasavietz-Gal4,UAS-CD8:GFP*.

B. Injecting depolarizing current into an LN with a ventrolateral soma evokes a train of spikes in that LN, and a much smaller depolarization in a simultaneously recorded PN. PN response is an average of 50 traces.

C. Injecting depolarizing current into a different LN (here with a dorsal soma) evokes hyperpolarization in a simultaneously recorded PN.

D. Spontaneous activity in a *krasavietz* LN with a ventrolateral soma. IPSPs (arrowhead) and short spikes (arrow) are characteristic features of these LNs. This is the same LN as in (B).

E. Spontaneous activity in a *krasavietz* LN with a dorsal soma. This is the same LN as in (C).

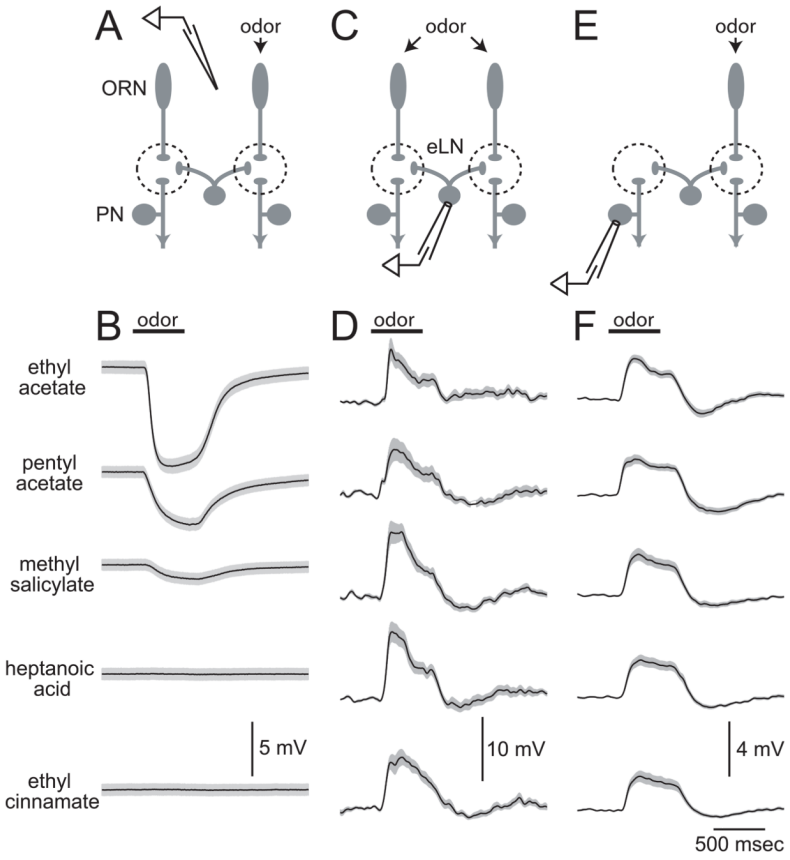

Figure 3. Comparing ORN activity, eLN activity, and lateral excitation in PNs

A. An electrode in the antenna records the extracellular local field potential, a measure of total ORN activity.

B. Antennal local field potential responses to a panel of odors which activate the ORN population to various degrees. A downward field potential deflection indicates increased ORN activity. Traces are averages of 8 recordings, ± SEM across recordings. Genotypes are the same as those used for panels D and F (4 *krasavietz-Gal4,UAS-CD8:GFP* and 4 *NP5221-Gal4,UAS-CD8:GFP*).

C. Activity in eLNs is recorded in whole-cell current-clamp mode.

D. All test odors elicit depolarization in eLNs. Traces are low-pass filtered to remove spikes, averaged across 8 cells, ± SEM across cells. All eLNs we recorded were disproportionately sensitive to the weaker odors and were broadly tuned. All these stimuli elicited similar spike rates as well as similar levels of depolarization. Genotype is *krasavietz-Gal4,UAS-CD8:GFP*.

E. Lateral excitation in PNs is recorded in whole-cell current-clamp mode. Direct ORN input to these PNs is abolished by bilaterally removing the olfactory organ (antenna or palps) containing the ORNs presynaptic to these PNs; the other organ is left intact and is stimulated with odors.

F. Lateral excitation evoked by the same odor panel. Traces are low-pass filtered to remove spikes, averaged across 12 cells, ± SEM across cells. Data from three glomeruli are pooled (VC1, VC2, DM1). Note the sensitivity and broad tuning of lateral excitation. Genotype is *NP5221-Gal4,UAS-CD8:GFP*.

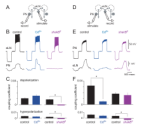

Figure 4. Connections between eLNs and PNs

A. Stimulating an eLN while recording a response in a PN. (Antenna are removed.) Genotype is *krasavietz-Gal4,UAS-CD8:GFP*.

B. In a typical control pair, hyperpolarizing and depolarizing the eLN (top) produces hyperpolarization and depolarization in the PN (bottom). Adding Cd^{2+} does not weaken the response, and indeed the response is slightly increased, probably because Cd^{2+} blocks spontaneous IPSPs and so increases eLN excitability. (Blue and black traces are from the same pair.) In a typical pair from a *shakB*^{2} mutant (magenta), PN responses are abolished. Top traces are single trials, bottom traces are averages of 40–70 trials.

C. Group data showing mean coupling coefficients (± SEM). The coupling coefficient is the change in the membrane potential of the postsynaptic cell, divided by the change in the presynaptic cell. Coupling is not significantly affected by Cd^{2+} (n=6 pairs tested with Cd^{2+}, paired t-tests) but is significantly decreased in the mutant (n=37 control pairs and 19 *shakB*^{2} pairs, p<0.0001, Mann-Whitney U-tests).

D. Stimulating a PN while recording the response in an eLN.

E. Hyperpolarizing and depolarizing a PN (top) produces hyperpolarization and depolarization in an eLN (bottom). Cd^{2+} weakens the response to depolarization but not hyperpolarization. (Blue and black traces are from the same pair.) In a typical pair from a *shakB*^{2} mutant, the response to hyperpolarization is absent, but the response to depolarization remains.

F. Group data showing that Cd^{2+} significantly reduces the response to depolarization (n=6 pairs tested with Cd^{2+}, p<0.05, paired t-test) but not hyperpolarization. The mutation eliminates the response to hyperpolarization (n=39 control pairs and 19 *shakB*^{2} pairs, p<0.0001, Mann-Whitney U-tests) but not depolarization.

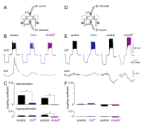

Figure 5. Connections between eLNs and iLNs

A. Stimulating an eLN while recording a response in an iLN. (Antenna are removed.) Genotype is *krasavietz-Gal4,UAS-CD8:GFP*.

B. Hyperpolarizing and depolarizing an eLN (top) produces hyperpolarization and depolarization in the iLN (bottom). Adding Cd^{2+} blocks most of the response to depolarization but not the response to hyperpolarization. (Blue and black traces are from the same pair.). In the *shakB*^{2} mutant pair, iLN responses are gone.

C. Group data showing that Cd^{2+} significantly reduces the response to depolarization (n=6 pairs tested with Cd^{2+}, p<0.005, paired t-test) but not hyperpolarization. The *shakB*^{2} mutation eliminates responses to both hyperpolarizing and depolarizing steps (n=39 control and 25 *shakB*^{2} pairs, p<0.0001, Mann-Whitney U-tests).

D. Stimulating an iLN while recording a response in an eLN.

E. In one sample pair, hyperpolarizing and depolarizing an iLN produces little effect in the eLN. Because Cd^{2+} blocks spontaneous IPSPs in the postsynaptic cell, it makes it easier to see a small degree of electrical coupling (blue, same pair). In a different pair (middle black traces), depolarizing the iLN produces relatively strong hyperpolarization in the eLN, implying a GABAergic connection. In a *shakB*^{2} mutant pair (purple), a strong inhibitory connection can still be observed from the iLN to the eLN.

F. There is no significant effect of either Cd^{2+} (n=6 pairs, paired t-tests) or the *shakB*^{2} mutation (n=39 control and 25 *shakB*^{2} pairs, Mann-Whitney U-tests) on iLN-to-eLN synapses. The failure to see significant results in the group data may reflect the heterogeneity of these connections.

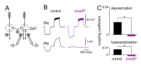

Figure 6. Connections between PNs

A. Recording simultaneously from two PNs in glomerulus DA1. Genotype is *Mz19-Gal4,UAS-CD8:GFP*. In control flies, sister PNs are coupled by mixed chemical-electrical synapses (Kazama and Wilson, 2009).

B. Hyperpolarizing and depolarizing a PN (top) produces hyperpolarization and depolarization in the other PN. In the *shakB*^{2} mutant, both hyperpolarizing and depolarizing responses are abolished.

C. Group data showing that coupling coefficients for both depolarizing and hyperpolarizing pulses are significantly reduced in the mutant (n=4 control and 4 mutant pairs yielding 8 coupling coefficients for each condition, $p<0.0005$, Mann-Whitney U-tests).

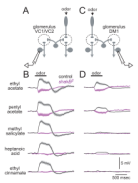

Figure 7. The *shakB*^{2} mutation abolishes odor-evoked lateral excitation in PNs

A. Recording lateral input to PNs in identified glomeruli (VC1 and VC2). Both of these glomeruli normally receive ORN input exclusively from the maxillary palp, and in these experiments the palp is removed. Thus, any odor-evoked input must reflect lateral input via LNs. Genotype is *NP5221-Gal4,UAS-CD8:GFP*.

B. In control flies, odors elicit lateral excitation in these PNs but in *shakB*^{2} flies, this is abolished (mean ± SEM, n=7 control cells and 7 mutant cells, p<0.001 for all odors, Mann-Whitney U-tests). A small amount of lateral inhibition remains in the mutant. Here results for VC1 and VC2 PNs were pooled because the two PN types exhibit similar amounts of odor-evoked lateral excitation (n=4 VC1 and 3 VC2 for both control and mutant).

C. Same as A, but for glomerulus DM1. This glomerulus receives ORN input exclusively from the antenna, and in these experiments the antenna is removed. Genotype is *NP5221-Gal4,UAS-CD8:GFP*.

D. Same as B, but for DM1 (mean ± SEM, n=5 control and 5 mutant, p<0.05 for all odors except the last, Mann-Whitney U-tests). Note that in control flies, the magnitude of lateral excitatory input to this PN is unusually small. This is not a general feature of antennal PNs, because in the same recording configuration many antennal PNs show large lateral excitation (Olsen et al., 2007).

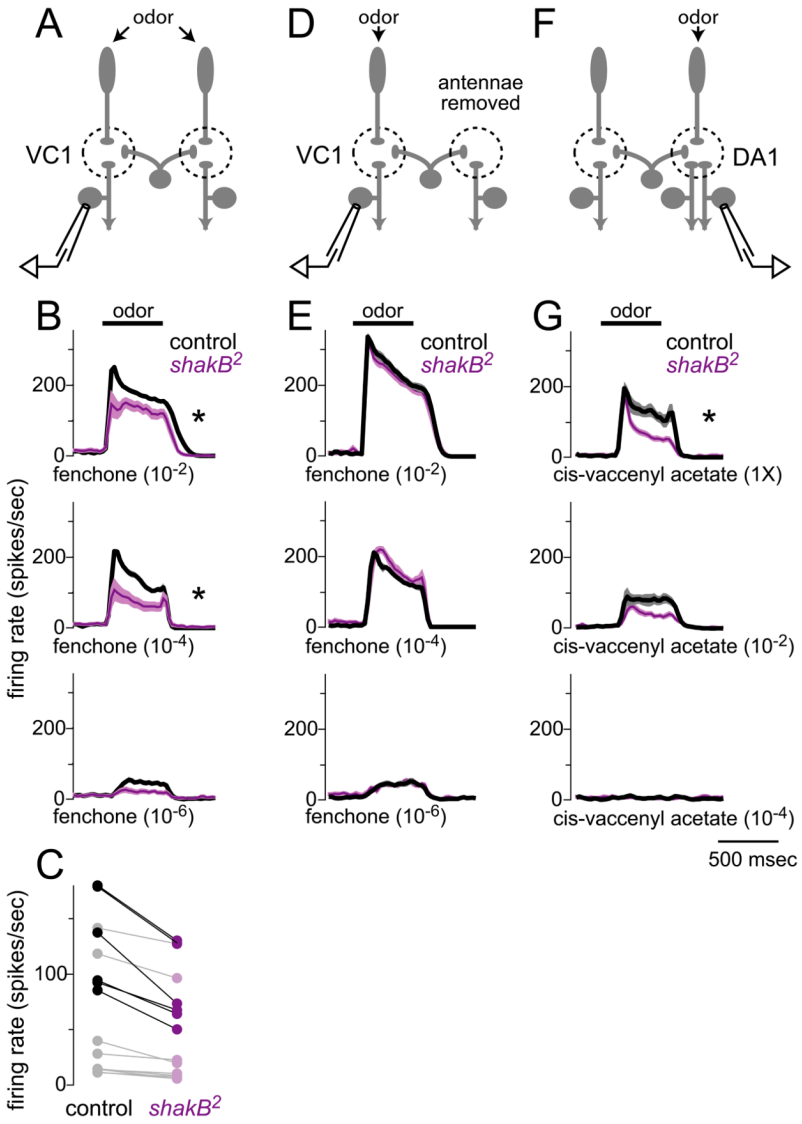

Figure 8. The *shakB*^{2} mutation reduces some PN odor responses

A. Recording odor-evoked spiking activity from VC1 PNs in an intact circuit.

B. Peri-stimulus time histograms show spiking responses of VC1 PNs to one test odor (fenchone) at three concentrations. Responses from control and *shakB*^{2} flies are overlaid (n=8–9 control and 6–8 mutant). Asterisks indicate significant differences (p<0.05, Mann-Whitney U-tests).

C. Comparison between mean odor-evoked firing rate (averaged across VC1 PNs) for every test odor. Responses in dark shades are significantly different (fenchone 10^{-2}, fenchone 10^{-4}, cyclohexanone 10^{-2}, cyclohexanone 10^{-4}, isoamyl acetate 10^{-2}, 4-methylphenol 10^{-3}); responses in pastel shades are not (fenchone 10^{-6}, heptanone 10^{-2}, heptanone 10^{-4}, heptanone 10^{-6}, cyclohexanone 10^{-6}, isoamyl acetate 10^{-4}, isoamyl acetate 10^{-6}, 4-methylphenol 10^{-1}, 4-methylphenol 10^{-2}).

D. Recording odor-evoked spiking activity from VC1 PNs with antennae removed. This makes fenchone a “private” odor for VC1 ORNs because these are the only palp ORNs that respond to fenchone.

E. Responses to fenchone in VC1 PNs recorded in flies with antennae removed (n=6 control and 5 mutant). There are no significant differences between control and mutant (Mann-Whitney U-tests).

F. Recording odor-evoked spiking activity from DA1 PNs. The odor which stimulates DA1 ORNs (cis-vaccenyl acetate) is relatively selective. Note that there are many PNs in this glomerulus.

G. Responses to cis-vaccenyl acetate in control and mutant DA1 PNs (n=5 control and 7 mutant). Asterisk indicates a significant difference (p<0.05, Mann-Whitney U-test).

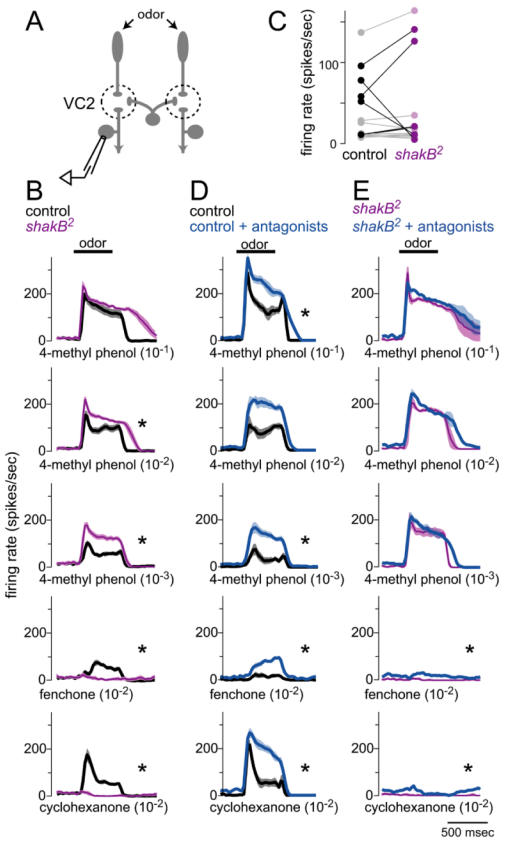

Figure 9. The *shakB*^{2} mutation impairs the recruitment of inhibition

A. Recording odor-evoked spiking activity from VC2 PNs.

B. Responses to several test odors in control and *shakB*^{2} VC2 PNs (n=6 control and 6 mutant cells). Asterisks indicate significant differences (p<0.05, Mann-Whitney U-tests).

C. Mean odor-evoked firing rate (averaged across VC2 PNs) for every test odor. Responses in dark shades are significantly different (fenchone 10^{-2}, fenchone 10^{-6}, heptanone 10^{-6}, cyclohexanone 10^{-2}, 4-methylphenol 10^{-2}, 4-methylphenol 10^{-3}); responses in pastel shades are not (fenchone 10^{-4}, heptanone 10^{-2}, heptanone 10^{-4}, cyclohexanone 10^{-4}, cyclohexanone 10^{-6}, isoamyl acetate 10^{-2}, isoamyl acetate 10^{-4}, isoamyl acetate 10^{-6}, 4-methylphenol 10^{-1}).

D. Most responses in control VC2 PNs are disinhibited after adding GABA receptor antagonist (5 μM picrotoxin and 20 μM CGP54626). Asterisks indicate significant smaller than in control files (n=4 cells tested with antagonists, p<0.05, paired t-tests).

E. In *shakB*^{2} VC2 PNs, the amount of disinhibition was significantly smaller than in control flies (n=5 odor stimuli, p<0.005, comparing differences in firing rates averaged across 4 control cells versus 4 mutant cells, paired t-test).